REMOTE MEASUREMENT AND PREDICTION OF BREAKING WAVE PARAMETERS

B. Robertson[1], I. Nistor[2], K. Hall[3], B. Buckham[4]

The analysis of wave breaking in shallow water has been on-going for almost 150 years. Numerous research papers have been published that investigate methods to predict breaking conditions and the geometric characteristics of breaking waves. This study presents a novel, safe, and low cost method to extract breaking wave properties from irregular waves in the surf zone, using optical and in-situ measurement systems. Sensitivities studies on methods of measuring the breaking water depth are compared and the water depth at the wave trough depth, corrected for optical offsets using a still water correction of 1/3 wave height, is found to be exhibit the least variability. A new effective seafloor slope definition, based on individual breaking wavelength to depth ratios, was found to increase predictive ability over previously variable seafloor slope extraction methods. Collected field data is compared against established breaking wave height formulas with general exponential form consistently finding best correlation. An optimized breaking wave height predictor featured a root mean square relative error of only 1.672% against the measured dataset. Finally, the study of the geometric shape of the plunging wave vortex as a possible indicator for the breaking intensity of ocean waves has been ongoing for almost 50 years with limited success. The validity of using the vortex ratio and vortex angle as a method of predicting breaking intensity is examined. Through the first complete analysis of field collected irregular wave breaking vortex parameters it is illustrated that the vortex ratio and vortex angle cannot be accurately predicted using standard breaking wave characteristics and hence are not suggested as a possible indicator for breaking intensity

Keywords: breaking waves; remote sensing; wave measurement; vortex parameters; breaker index; surf similarity parameter

INTRODUCTION

The breaking of shallow water ocean waves is one of the most important elements in coastal engineering design. Shallow water waves create large impact forces on coastal structures, drive sediment transport, regulate a number of biophysical and air-sea chemical processes, and ultimately control coastal morphology and storm inundation. As a result, the value of accurate measurements and prediction systems for breaking waves cannot be overstated - it is paramount to any planning or design concerning the surf zone. This study presents a novel, low cost method to extract the necessary accurate and precise breaking wave conditions to help find this data need.

Breaking wave studies are generally completed using laboratory flumes, large scale field research programs or in numerical environments (Goda, 2010; Rosati et al., 1990; Shand et al., 2012; Smith and Kraus, 1991). Unfortunately, laboratory investigations of breaking waves are often based on regular or monochromatic waves, rather than more realistic irregular wave systems (See Table 2) and are inherently limited by tank dimensions (Robertson et al., 2013a).

In nature, physical measurements of individual waves are complicated by the wide spectrum of incoming heights, periods, and directions and the wide spatial area of breaking. As a result, it is extremely difficult to mount in situ point measurement devices at exact breaking positions. Arrays of photopoles (Ebersole and Hughes, 1986), resistive wave gauges (Black and Rosenberg, 1992), seafloor mounted pressure sensors (Birkemeier et al., 1997) and Acoustic Doppler Current Profilers (ADCP) have all been used to measure near-shore waves. The relatively low spatial resolution of these methods, constantly changing seafloor slopes, necessity of good breaking conditions, and researcher safety are often cited obstacles for field investigations of breaking waves. While numerical simulations of breaking waves from new computational fluid dynamics codes, such as Smoothed Particle Hydrodynamics, indicate huge potential for future investigative work, they are generally only qualitatively validated due to lack of detailed full scale data (Khayyer et al., 2008).

Positively, recent advances in video remote sensing have allowed for excellent spatial resolution of individual breaking position, wave height and period (de Vries et al., 2010; Gal et al., 2011; Shand et al., 2012). Through the integration of remotely sensed wave heights and positions, with site specific seafloor bathymetric surfaces and directly measured shallow water incoming wave conditions, this

[1] Mechanical Engineering, University of Victoria, 3800 Finnerty Rd, Victoria, Canada, bryson@uvic.ca
[2] Civil Engineering, University of Ottawa, 75 Laurier Ave, Ottawa Canada, inistor@uottawa.ca
[3] Office of Research, University of Newcastle, University Dr, Callaghan, Australia, kevin.hall@newcastle.edu.au
[4] Mechanical Engineering, University of Victoria, 3800 Finnerty Rd, Victoria, Canada, bryson@uvic.ca

novel study presents a novel, low cost, robust, and repeatable method to directly measure all the necessary parameters, which affect breaking wave characteristics, from the surf zone. These include breaking wave height, breaking water depth, wave period, and effective seafloor slope.

Additionally, breaking waves are generally differentiated as spilling, plunging or collapsing waves. In an effort to further differentiate between waves in the plunging category and predict the "intensity" of a breaking wave event, Longuet-Higgins (1982) proposed fitting a cubic function to the breaking vortex profile of a plunging wave (see Figure 4). He postulated that the ratio of the vortex length to vortex width may describe the 'intensity' of a plunging wave breaking event and remained constant at 2.75. Utilizing the collected profile images on individual breaking waves, this study thoroughly investigates the validity of using the vortex parameters as methods of predicting breaking intensity.

In this paper, the experimental collection techniques are overviewed, including new methods to correlate the breaking wave conditions to those found just prior to the surf zone. Methods for extracting wave heights and surf zone periods are presented, and novel definitions for the water depth at breaking and the effective seafloor slopes are described and quantitatively reinforced. The collected data is compared against published breaking wave height predictors to illustrate the high degree of correlation with most recently published predictors. Finally, the best fitting published relationship is optimized to determine better possible correlations with measured data.

REMOTE COLLECTION OF BREAKING WAVE PARAMETERS

Shallow water breaking waves are heavily affected by incoming wave characteristics and local bathymetric conditions. A number of detailed datasets are required to quantify the effects of local conditions on breaking waves; bathymetric surveys of the surf zone and surrounding seafloor, detailed measurements of both incident and breaking wave characteristics, geographic positions of breaking waves and geometric profile of each wave are required.

The most important step in studying shallow water breaking waves is study location choice. Uncontrollable and complicating effects of localized winds, wave/wave interactions, wave reflection, and currents should be minimized. For this study, The Hook and Sewers Peak in Santa Cruz, California and Tropicana Beach in Barbados were determined have the correct mix of wave climate, local geographic features, access to scientific facilities and ease of access to collect the necessary measurements.

Surf Zone Bathymetry

Seafloor slope has been proven to be a major determining factor in the breaking depth, height and geometric shape of waves (Couriel et al., 1998; Grilli et al., 1997). In order to negate any temporal variation in seafloor profiles during the study, only locations with permanent coral or rock seafloor geology were examined at each location.

For the Santa Cruz region, the United States Geological Survey (USGS) provided bathymetric survey results from the California Coastal Mapping Project. Using a 234.5 kHz sidescan sonar, the survey mapped the entire Santa Cruz region from approximately ~0.5m to 100 m depth. The sonar featured a vertical depth resolution of 0.1 m at 57 m depth and of 0.3 m at 171 m depth. Tidal data was collected from the National Ocean and Atmospheric Administration (NOAA) tide gauges.

For Tropicana Beach in Barbados, the Barbados Government Coastal Zone Management Unit provided Light Detection and Ranging (LIDAR) data from their West coast beaches. Additional shallow bathymetric surveys were completed over a 500m X 500m area within the surf zone using a 38/200 kHz single beam echosounder. Tidal data was collected using a tide gauge located in Bridgetown Harbour (located at 13.11° N, 59.63° W).

Incoming Wave Characteristics

In order to collect data on incoming wave conditions and characteristics, a 1200 kHz acoustic Doppler current profiler (ADCP) was mounted just offshore of the surf zone, in 4 to 8 m of water. The ADCP collected continuous data of the entire water column using 0.05 m vertical cells and a 0.25 sec ping rate during the periods of study. Post-processing removed spurious complicating frequencies from the surface track data via a Fast Fourier Transform and band pass filter. The band pass filter used a $0.5F_{sig}$ for low frequency cut off and $6F_{sig}$ for a high frequency cut off (Mase and Iwagaki, 1982).

Individual incoming wave heights (*H)* were extracted from the raw free surface trace data using both a zero up and zero down crossing method. Individual wave periods (*T*) were additionally calculated using a wave crest to wave crest methodology. Significant wave heights (H_{sig}), frequencies (F_{sig}), and directions (D_{sig}) were automatically calculated at 5 min intervals using overlapping 20 min record lengths. The 5 min interval measurements allowed for additional time domain resolution to be extracted from statically robust sliding 20 min wave measurement interval.

Breaking Wave Characteristics

The extraction of wave characteristics at the instant of breaking is a non-trivial matter. Using numerous high definition video cameras, installed by CoastalCOMS Ltd, the University of California at Santa Cruz and the USGS, excellent oblique video of the study zones was collected. The Hook camera was located at 39.9610° N, 109.9635° W, at an elevation of 14.44 m above mean low lowest water (MLLW) level, whereas the Sewers Peak camera was located at 39.9568° N, 109.9710° W, at an elevation of 14.55 m above MLLW. In Barbados, a self-contained high definition video camera was securely mounted 4.54 m above Lamont zero water level, at 13.2194° N, 59.6421° W.

The extraction of wave position and height data from an overview video camera image required that the oblique image is rectified to the horizontal plan, and then geographically corrected according to the four ground control points (GCP). This georectification process is highly affected by tidal levels, thus each wave image required individual tidal level measurements and an individual transformation matrix. The end result of the georectification process was direct knowledge of the true latitude and longitude locations of every pixel within the oblique overview images (See Figure 1).

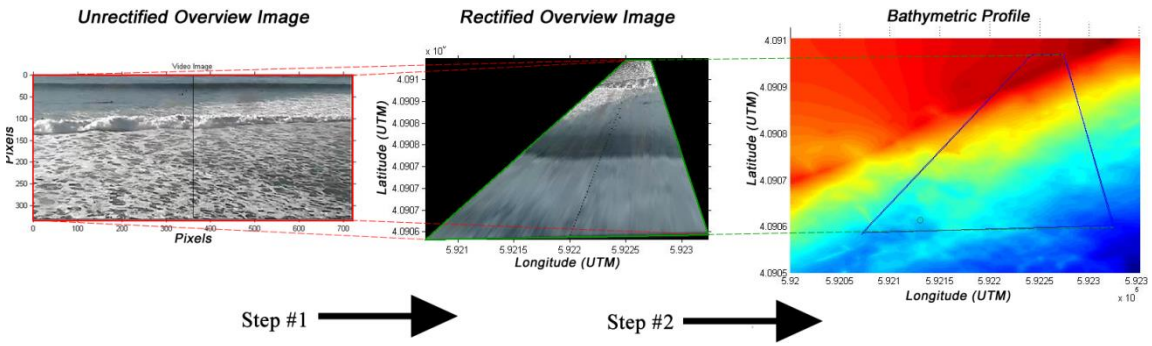

Figure 1: Georectification process flow diagram

The accuracy of the rectification process was quantified by comparing known locations against those calculated using pixel locations in the rectified image. Average offset variations of 1.58 m, 1.60 m and 3.8 m were calculated for the Hook, Sewers Peak and Tropicana Beach respectively. Given that the reported accuracy of the GPS was 3 m, these uncertainty magnitudes are not significant.

Wave Height Extraction

Automatic extraction of breaking wave heights from video data is currently ongoing (de Vries et al., 2010; Shand et al., 2012), yet all published methods identify significant numbers of false positive wave height readings in the automatic algorithms. As a result, manual methods were employed in this study to identify wave crest and trough locations. Wave crest locations (X) were indicated by the

appearance of white water, while the associated wave trough pixel (O) was identified by assessing the trough impact location of the breaking wave jet (See Figure 2).

Figure 2: Wave crest and trough identification

The wave height at breaking (H_b) was calculated using Eq. (1), a known camera tilt angle (θ_c) and wave crest (x_c) /trough (x_t) real world coordinate positions:

$$H_b = (x_c - x_t)\tan(90 - \theta_c) \quad (1)$$

The wave trough and crest pixel locations were manually selected and thus subject to human error. For The Hook and Sewers Peak, average height uncertainties were calculated to be 2.3% and 3.9% at The Hook and Sewers Peak respectively. For Tropicana deployments, the 12" validation buoy height uncertainties varied between 2.1 % and 3.3%.

Breaking Depth Extraction

The breaking depth was extracted from the bathymetric depths at the tidally corrected, real world breaking positions of each wave (see Step 2 in Figure 1). Unfortunately, the exact definition of the water depth, when a wave front become vertical and breaks, varies between published authors and papers. Blenkinsopp and Chaplin (2008), Black and Rosenburg(1992), Kamphuis(1991) and Smith and Kraus(1991) all used different definitions and techniques. For this experiment, three different methods were used and later compared to determine which provided the best performance:

1. Water depth at wave trough pixel (h_t): h_t is directly extracted from the bathymetric model, using the pixel position at the optical wave trough position.
2. Corrected water depth at trough(h_c): In order to account for the fact that wave troughs are generally located below the SWL(Flick et al., 1981; Le Mehaute, 1976), Shand et al. (2012) suggests using $h_c = h_t + 1/3*H_b$ for water depth measurements.
3. Set down corrected water depth (h_{sd}): Longuet-Higgins(1963) determined that individual shallow water waves induce shoreward currents, creating a consistent water level set down at the break point. Longuet-Higgins suggested using Eq. (2) to account for this effect. The effect of wave set down has previously been assumed negligible in published studies (Shand et al., 2012). However given that the mean wave induced set down was calculated to be 0.120 m, 0.15m and 0.09m at the Hook, Sewers Peak and Tropicana Beach respectively, they were deemed significant enough to warrant further analysis.

$$\eta = -\frac{1}{8}\frac{H^2(2\pi/L)}{\sinh(4\pi h/L)} \quad (2)$$

Wave Period Extraction

In order to analyze the effect of individual wave periods on the breaking characteristics, three different incoming wave period definitions and two breaking zone period definitions were compared. For the incoming wave period, a zero down, zero up and crest-to-crest analysis was performed on the ADCP surface track data. However, the breaking wave period extraction required a consistent shoreward, post breaking location and a timestack (de Vries et al., 2010; Gal et al., 2011; Lippmann and Holman, 1991; Shand et al., 2012) of the oblique overview video. By identifying when individual waves pass the consistent fixed location, individual wave periods were calculated by measuring the number of pixels between each wave crossing and multiplying by the frames per second (fps) speed of

the video. Two methods of quantifying the breaking period were used: the time between the wave of interest and both the preceding and proceeding waves.

A direct comparison of the different wave period definitions (three incoming and two breaking) indicated the lowest variation between incoming and breaking wave periods was found using the incoming crest to crest period and preceding breaking wave period. Thus, these two parameters were used for the remainder of the analysis. See Robertson *et al* (2013b) for additional details.

Effective Seafloor Slope

The bathymetric slope plays a significant role in determining the breaking wave height, depth, and shape (Couriel et al., 1998). The slope is a function of wave direction, wave ray method (curved or straight), and a relevant geographical distance. The slopes reported in published field studies vary between coastline approach slopes to instantaneous laboratory bar slopes. The Coastal Engineering Manual(CEM) (CERC-EW, 2008) recommend that *"for non-uniform beach slopes, the average bottom slope from the break point to a point one wavelength offshore should be used".*

In order to determine if improved predictive performance could be achieved through an *effective* seafloor slope, the CEM method was compared against wavelength-dependent effective slope definitions. The following effective slopes were calculated along the curved wave rays: (See Figure 3)

$$m_{1/2} = \frac{\left(h_b + \frac{L_b}{2}\right)}{x_{1/2}} \quad (3) \qquad m_{1/3} = \frac{\left(h_b + \frac{L_b}{3}\right)}{x_{1/3}} \quad (4) \qquad m_{1/4} = \frac{\left(h_b + \frac{L_b}{4}\right)}{x_{1/4}} \quad (5)$$

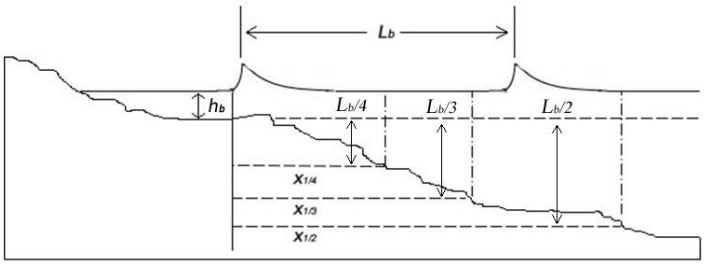

Figure 3: Effective slope diagram

Wave Vortex Parameters

The final parameter for this study was the breaking vortex ratio and vortex angle. Capturing breaking wave profile images from irregular waves under field conditions proved to be more difficult than initially expected. However, through both in-water videography and land-based photography, sufficient high quality images were captured and used to extract vortex parameters.

First, each individual vortex profile image was correlated to its corresponding breaking wave in the timestack image by using the digital time metadata from the vortex profile image and the overview camera. Wave profile images were then imported into ImageJ (Rasband, 1997 - 2012) and cubic functions were fitted using four defining vortex points: the point of intersection of the wave jet and wave trough (point #1), the vortex "turn-over" point (point #2), and the two points of maximum vortex width (point #3 & #4). Figure 4 gives a visual illustration of the four defining points.

The ratio between vortex length (l_c) and vortex width (W_c), *Y*, were then calculated and the vortex angles were corrected to be lower than 90°. It should be noted that marginally oblique views will result in reported vortex ratios being slightly lower than a true perpendicular profile while localized winds will cause the vortex cavity to collapse or expand depending on wind directions. See Robertson (2013) for additional discussion.

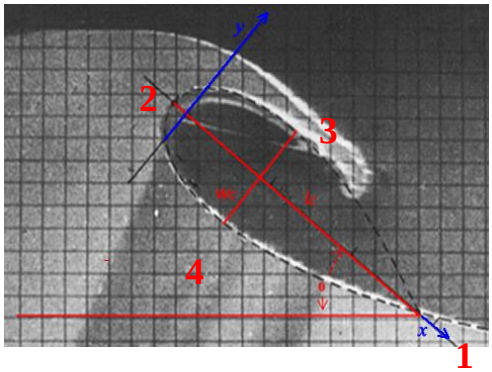

Figure 4: Cubic fitting of the enclosed vortex and the four defining points. (Altered image from Longuet-Higgins (1982))

Breaking Wave Dataset Overview

In total, 28 hours of data were collected and analyzed. The required wave characteristics for inclusion as a valid data point in the final database included wave height, water depth, wave period, wave vortex ratio and vortex angle. Table 1 gives a brief overview of the mean, maximum and minimum wave characteristics for the entire collected dataset.

Table 1: Study data overview

	Hook, Santa Cruz			Sewers, Santa Cruz			Tropicana, Barbados		
	Min	Mean	Max	Min	Mean	Max	Min	Mean	Max
Number of Waves		67			35			85	
Wave Heights (m)	0.89	2.07	3.03	1.33	2.52	3.51	1.20	1.52	2.16
H_c Depths (m)	0.98	2.19	2.76	1.19	2.54	3.46	1.01	1.59	2.56
Trough Depths (m)	0.89	2.00	2.55	0.75	1.77	2.27	0.71	0.98	1.34
Wave Periods (sec)	9.7	16.1	20.4	9.2	15.7	23.5	8.3	10.3	12.0
Slope - CEM	0.013	0.026	0.038	0.003	0.026	0.039	0.026	0.042	0.066
Slope - $m_{1/3}$	0.012	0.018	0.022	0.021	0.024	0.030	0.038	0.046	0.049

To the best of the author's knowledge, the collected database of breaking wave profiles and vortex parameters is unique within the academic sphere and the perhaps most detailed ever collected from field conditions. This dataset allowed for a complete analysis of breaking wave prediction methods and vortex ration "intensity" categorizations.

BREAKING WAVE HEIGHT PREDICTOR

The wave height at breaking is one of the most essential measurements required for surf zone analysis and a substantial number of publications focus on its prediction (Rattanapitikon and Shibayama, 2000; Robertson et al., 2013a). While non-exhaustive, many of the frequently cited breaker height predictors are presented in Table 2. With the exception of Weggels' 1972 and Smith and Kraus' updated 1991 version, the relationships used for comparison do not rely on the offshore wave height (H_o) due to non-linear depth based effects of refraction, diffraction and shoaling.

Prior to investigations of the predictive ability of the equations in Table 2, it is necessary to identify the best techniques to quantify the breaking depth and effective seafloor slope. Throughout the following analyses, verification results are analysed using the direct comparison root mean square error (RMSE) and root mean square relative error (ER) values (Rattanapitikon and Shibayama, 2000).

Table 2: Overview of published breaking wave height predictors

Author, Date	Primary Relationship	Applicability
McCowan, 1894	$H_b = 0.78h_b$	m = o, $\eta_c = 1.78h_b$
Battjes, 1974	$H_b = (1.062 + 0.137\log(\xi_o))h_b$ Where: $\xi_o = \tan\alpha/\sqrt{H_o/L_o}$	$0.05 < m < 0.2$
Weggel, 1972	$H_b = h_b\left[b(m) - a(m)\frac{H_0}{gT^2}\right]$ $a(m) = 43.8(1.0 - e^{-19m})$ $b(m) = 1.56(1.0 + e^{-19.5m})^{-1}$	$1/50 < m < 1/5$ $\frac{H_0}{L_o} \leq 0.06$ $\eta_c = 1.78h_b$
Ostendorf and Madsen, 1979	$H_b = 0.14L_b\tanh\left((0.8 + 5m)\,2\pi h_b/L_b\right)$	$m < 0.1$
Smith and Kraus, 1991	$H_b = h_b\left[b(m) - a(m)\left(\frac{H_0}{L_0}\right)\right]$ Where: $a(m) = 5.00(1.0 - e^{-43m})$ $b(m) = 1.12/(1.0 + e^{-60m})$	$0.0125 < m < 0.1$ $0.0007 < \frac{H_o}{L_o} < 0.0921$
Rattanapitikon Shibayama, 2000	$H_b = 0.17L_o\left(1 - e^{\left(\frac{\pi h_b}{L_o}(16.21m^2 - 7.07m - 1.55)\right)}\right)$	$0 \leq m \leq 0.44$ $0.001 < \frac{H_o}{L_o} < 0.1$
Goda, 2010	$H_b = 0.17L_o\left(1 - e^{\left(\frac{-1.5\pi h_b}{L_o}\left(1 + 11m^{\frac{4}{3}}\right)\right)}\right)$	$0.005 \leq m \leq 011$
Seyama and Kimura, 1988	$H_b = \left(0.16L_o\left\{1 - \exp\left(-0.8\pi\, h_b/L_0\left[1 + 15m^{\frac{4}{3}}\right]\right) - 0.96m + 0.2\right\}\right)$	$0.02 < m < 0.1$
Kamphuis, 1991	$H_{sb} = [0.095\exp(4.0m)]L_b\tanh\left(2\pi h_b/L_b\right)$	Undetermined

Breaker Depth Analysis

In order to assess the best definition of breaking depth, the three variations of breaking were first plotted against the breaker height for all locations. As shown in Table 3, h_c displayed the lowest RMSE and highest correlation (R^2 = 0.84). This was expected since h_c accounts for optical variation in the wave trough location and agrees with the numerical theory of Lin *et al.* (1998) and wave flume experiments of Flick (1981).

Table 3: Breaker depth analysis details

Location	Breaking Height vs. Breaking Depth				
		Constant (m)	Rgs Slope	RMSE (m)	Robust R^2
All Waves	Wave Trough	0.56	0.96	0.27	0.75
	Corrected Depth	-0.14	1.04	0.22	0.84
	Setdown Depth	0.21	0.91	0.22	0.82

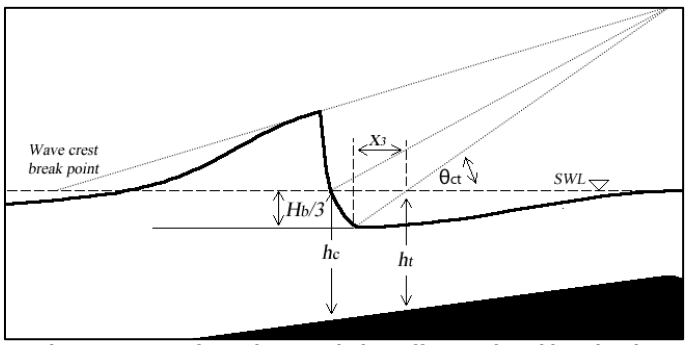

Figure 5: Wave face slope variation effect on breaking depth.

Further analysis was conducted to see if better correlation could be achieved by correcting for the front wave face slope. A plunging breaker generally does not exhibit a classical theoretical saw tooth shape but rather only the wave crest becomes vertical and the wave face features a non-vertical overall slope. A basic sensitivity study was conducted to determine if the wave face slope, and associated change in zero-crossing location, influenced the final correlations between breaking height and depth.

An optimized correlation was found to occur when the wave face slope resulted in a 30% additional horizontal distance before exacting the water depth (i.e. $1.3x_3$ as shown in Figure 5). The trend between breaker height and depth correction is shown in Figure 6. It is noted that each individual site exhibits very similar trend lines to the final fitted regression line, presented in Eq. (6).

$$H_b = 0.88h_b + 0.16 \quad (6)$$

Goda (2010) recognized a 14 % coefficient of variability (CoV) inherent within regular breaking waves, which are illustrated by the black dotted lines in Figure 6. He suggested an 18% - 23% CoV should be expected for irregular waves. In the current irregular wave study, an 18 % CoV captured more than 90 % of all measured data points. Given that these parameters were extracted from field sites using low cost, remote techniques, the CoV illustrates the comparative accuracy of using h_c to define the breaking depth.

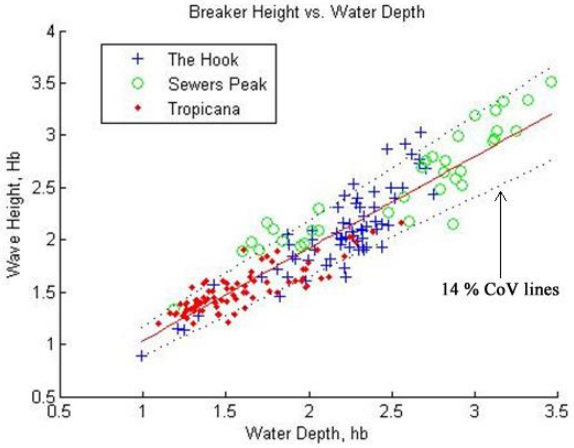

Figure 6: Relationship between breaker height and breaker depth for the three field sites.

Effective Seafloor Slope Sensitivity

In order to determine if the presented effective seafloor slope methods (Figure 3) improved predictive ability, their performance in the Goda 2010, Rattankipition and Shibayama 2000 , Kamphuis 1991 and Smith and Kraus 1991 equations was compared against those using the CEM slope method. As shown in Table 4, the breaking wave height was consistently better predicted using the effective seafloor slope methods. Using $m_{1/4}$ seems to consider a section of bathymetric profile that is too short to fully account for the breaking conditions, whereas $m_{1/2}$ seems to include a slope that plays a less dominant role in breaking conditions. It is shown that $m_{1/3}$ best represents the effective seafloor slope for breaking waves.

Table 4: Average R^2 values for the four different slope definitions.

Location	$m_{1/4}$ R^2	$m_{1/3}$ R^2	$m_{1/2}$ R^2	CEM Slope
Hook	0.81	0.80	0.79	0.80
Sewers Peak	0.79	0.82	0.82	0.80
Tropicana	0.73	0.77	0.76	0.61
Average	0.77	0.80	0.79	0.74

Performance of Breaking Wave Height Predictors

Through the choice of effective seafloor slope and breaking depth parameters defined above, it is possible to quantitatively determine the predictive ability of the relationships presented in Table 2. An overview of the linear regression parameters and the values associated with the direct comparison are shown in Table 5.

Table 5: Overview of the performance of published breaking wave height predictors

Methodologies	Robust Fit			Direct Comparison		
	Constant	Rgs Slope	Robust R^2	RMSE	Linear R^2	ER
McCowan, 1894	0.16	0.88	0.85	0.41	0.39	2.38
Battjes, 1974	1.03	0.40	0.83	0.66	0.00	3.02
Weggel, 1972	-0.06	1.02	0.76	0.26	0.76	1.88
Ostendorf and Madsen, 1979	-0.04	0.17	0.79	0.37	0.51	2.26
Smith and Kraus, 1991	-0.03	1.05	0.70	0.30	0.68	2.03
Rattanapitikon and Shibayama, 2000	0.02	0.18	0.82	0.24	0.79	1.81
Goda, 2010	-0.01	0.19	0.81	0.30	0.69	2.01
Seyama and Kimura, 1988	-0.06	0.35	0.78	0.90	0.00	3.52
Kamphuis, 1991	-0.01	0.14	0.81	0.65	0.00	2.99

Firstly, it is noted that the measured values find the best correlation (*ER* = 1.81%, RMSE = 0.24) with the wave height predictor of Rattanapitikon and Shibayama (2000). Godas' (2010) relationship shows good correlation with the measured dataset. Rattanapitikon and Shibayamas' equation follows a similar exponential functional form and reinforces the performance of this common exponential predictive form.

McCowan's (1894) relationship under predicted the measured wave height values. Given that all of the measured waves are of plunging type, the McCowan's constant of 0.78 may find better agreement with spilling waves. Battjes (1974) used the Surf Similiarity Parameter (SSP) as a parameter in describing the breaking height of waves yet his prediction performs poorly against the measured dataset. While Weggel (1972) attempted to only predict the maximum wave heights, the correlation between the predicted data and the regression fitted line is excellent. Ostendorf and Madsens'(1979) relationship under predicted breaking wave heights. Smith and Kraus (1991) updated the constants in Weggel's equation yet, as shown in Table 5, the recent constants find lower correlation with the dataset.

Kamphuis'(1991) irregular wave equation significantly under predicted. However, the wave heights predicted by Kamphuis equation averaged 30.3% lower than those measured. This is in accordance with the postulation by Goda (2010) that "*the incipient breaking height of the significant wave is about 30% lower than that of regular waves."* This is corroborated by the height predictions from the irregular wave formula of Seyama and Kimura (1988), which also fell well below the measured values.

Optimized Breaking Wave Height Predictors

Analysis of the ER and RMSE values in Table 5 and the functional forms of the equations in Table 2 indicates that the regular wave exponential form used by Rattanapitikon and Shibayama, 2000 and Goda, 2010 best predicts the breaking wave heights. The general exponential form can be described using (where K_g is an overall constant and K_{gm} is a slope based correction):

$$H_b = K_g L_o \left\{1 - \exp\left(\pi\, {h_b}/{L_0}\, K_{gm}\right)\right\} \tag{7}$$

Given the newly presented method for extracting effective seafloor slopes from field tests, additional analyses on the slope constant were completed to determine if better correlation could be achieved by following the optimization procedure presented in Rattanapitikon and Shibayama (2000). This optimization yielded a significant improvement in predictive ability (RMSE of 0.20 and an ER value of 1.67 %) through the use of Eq. (8).

$$H_b = 0.17 L_o \left\{1 - \exp\left(\pi\, {h_b}/{L_0}\, (1.978m - 1.792)\right)\right\} \tag{8}$$

Note that Eq. (8) was developed based on the measured data, which does not cover all possible breaking conditions, and should only be applied within the limits of the presented data.

WAVE VORTEX PARAMETERS AND BREAKING INTENSITY

Subsequent to the constant vortex ratio of 2.57 prediction of Longuet-Higgins (1982), field and flume based work (Blenkinsopp and Chaplin, 2008; Couriel et al., 1998) reported vortex ratio values vary between 1.73 and 4.43; depending on wave and seafloor characteristics. Mead and Black (2001) analyzed the previously published images of wave vortex ratios at 23 different plane and barred location worldwide and found that Eq. (9) gave an R^2 value of 0.71 to predict the vortex ratio (Y):

$$Y = 0.065m' + 0.821 \tag{9}$$

where $m' = m\cos\varphi$, m is the seafloor slope normal gradient and φ is the peel angle of the wave. Unfortunately, Mead and Black collected no direct quantitative wave data and consequently proposed that the vortex ratio is independent of wave characteristics and depends solely on seafloor slope. However, Blenkinsopp and Chaplin (2008) measured vortex ratios ranging from 1.46 to 2.28 on a constant slope of 1:10, thus indicating that slope is not the only factor effecting vortex parameters as predicted by Eq. (85).

In perhaps the most detailed study until this point, Johnson (2009) investigated trends between previous suggested vortex parameters and wave characteristics in a wave flume. Johnson noted that the vortex ratio increased with wave height and is unaffected by wave period. The data presented indicates that lower seafloor slopes do not affect the vortex ratio and that reef crest water depth plays a defining role in vortex shape. Unfortunately, Johnson was unable to explicitly quantify any trends due to low correlation values and noted that, *"the combined effects of wave height, period, water level, reef crest width and seaward reef slope on breaking intensity through the breaking wave vortex shape parameters, needs to be assessed".*

Vortex Ratio Analysis

For this study, initial analyses to determine vortex ratio dependencies focused on breaking wave height and the breaking water depth. As shown in Figure 7, a general trend of increasing the non-dimensional height resulted in reduced vortex ratios for the entire dataset. A very similar plot was produced for water depth and R^2 values of only 0.23 and 0.20, for wave height and water depth respectively, indicate the lower correlation levels. This contradicts the findings of Johnson (2009), who found smaller waves created lower vortex ratios.

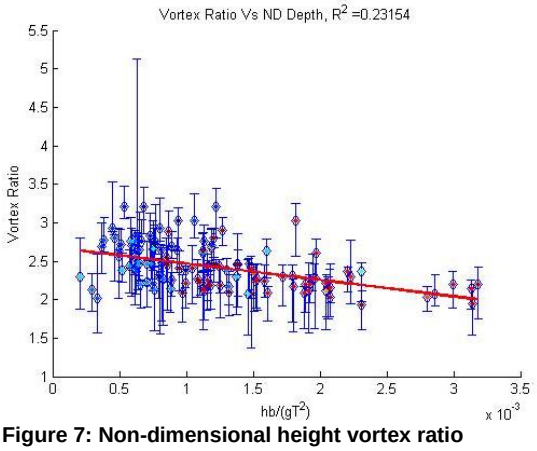

Figure 7: Non-dimensional height vortex ratio relationship

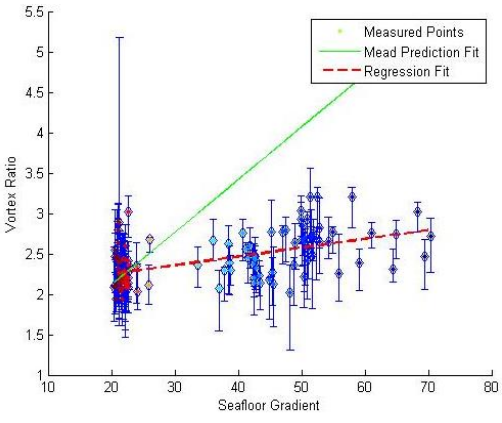

Figure 8: Wave vortex and effective seafloor slope relationship

When investigating the effect of breaking depth, each site displayed contradictory results. The Hook results indicated a positively sloped dependence, while Sewers Peak and Tropicana featured negatively sloped relationships. A similar set of conflicting relationships were found using the breaker height, thus possibly indicating a location dependence of vortex ratios.

As shown in Figure 8, increased effective seafloor slopes may result in larger vortex ratios. The large uncertainty levels, considerable amounts of scatter and the R^2 value of only 0.27 indicate the predicted trend is not definitive and may only be a function of the fitting algorithm (Eq. (9) is plotted to indicate the performance of Mead and Black's formula). There was no consistent response of the vortex ratio to seafloor bathymetry when comparing individual sites. The trend line fitted for the data points collected at Tropicana Beach displayed the opposite gradient dependence from to the entire dataset shown in Figure 8.

Many ocean enthusiasts qualitatively believe that increasing wave periods result in decreasing vortex ratios. However, the regression line in Figure 9 indicates that increasing wave periods result in small increasing vortex ratios. Yet an R^2 value of only 0.18 and the large uncertainty bars indicate no substantial dependence between the vortex ratio and wave period. No published studies have found correlation between period and vortex ratios.

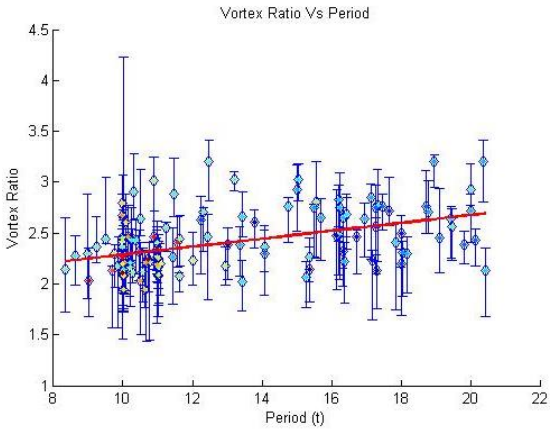

Figure 9: Wave vortex and wave period relationship

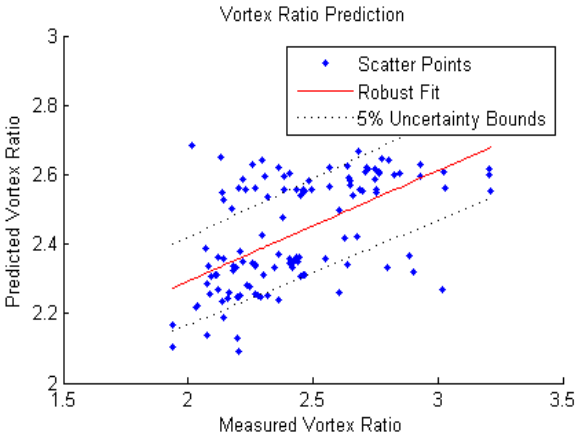

Figure 10: Predicted and measured wave vortex ratios.

As summarized in Table 6, the vortex ratio was rigorous analysed against all breaking wave and local bathymetric characteristics. No trend line found a correlation of determination above 0.28 and no defining relationships could be drawn from the collected data. This corroborates the findings of Johnson (2009), Blenkinsopp (2008) and Grilli *et al.*(1997) and brings into doubt the validity of Longuet-Higgins suggestion that breaker vortex ratios may be good descriptor of breaking intensity.

Table 6: Vortex Ratio Relationships Overview

	All Sites			
	Constant	Slope	R-Square	Linear RMSE
ND Depth	2.70	-210	0.23	0.26
ND Wave Height	2.80	-280	0.20	0.26
Seafloor Slope	2.80	-12.0	0.26	0.25
Breaker Index	2.00	0.39	0.11	0.28
Period	1.90	0.04	0.21	0.26
Breaker Steepness	2.80	-12.0	0.06	0.28
Breaking SSP	2.80	-0.97	0.14	0.27
Ursell Number	2.20	0.00	0.24	0.26

Given the lack of dependence of the vortex ratio on individual wave characteristics, an optimized non-dimensional multi-parameter approach data fit was completed. Eq. (10) achieved an R^2 value of 0.31. While Eq. (10) does find better correlation with the measured vortex ratios, considerable scatter was still evident in plotted results (See Figure 10) and only 70 % of all measured vortex ratios fall within 5 % of those predicted.

$$Y = 2.94 - 1.77\frac{H_b}{gT^2} + 12.12\frac{h_b}{gT^2} - 9.11m_{1/3} \tag{10}$$

It should be noted that there are numerous natural effects which will negatively affect the correlation between vortex ratios and wave parameters. Firstly, not every incident wave featured an enclosed vortex and wave induced water level set-up will create temporary non-accounted for increased water levels within the surf zone. Additionally, wind direction and speed alters the vortex shape of breaking waves. Onshore winds will generally increase the vortex ratio by decreasing the relative vortex width, while offshore winds will increase the vortex width, thereby lowering the vortex ratio.

Vortex Angle Analysis

Both Longuet-Higgins(1982) and Mead and Black(2001) suggested that the vortex angle, θ, may be another possible method to numerically categorize breaking wave events. Following the same procedure as above, the correlation between the vortex angle and various wave parameters is presented in Table 7. Unfortunately, none of the relationships featured an R^2 value above 0.02 and all featured significant RMSE.

Table 7: Vortex angle dependence overview

	Wave Vortex Angle Relationships			
	Constant	Slope	R-Square	Linear RMSE
ND Depth	47.0	-420	0.00	5.00
ND Wave Height	46.0	180	0.00	5.00
Seafloor Slope	45.0	54.0	0.02	4.90
Breaker Index	46.0	0.22	0.00	5.00
Period	48.0	-0.15	0.01	5.00
Breaker Steepness	43.0	84.0	0.01	5.00
Breaking SSP	44.0	5.60	0.02	4.90

The highest co-efficient of correlation values were found for seafloor slope and SSP plots, yet a basic visual analysis of Figure 11 and Figure 12 show the high degree of data scatter and a lack of dependence with respect to the independent variables. These findings corroborate previous laboratory investigations into breaker vortex angles which found no dependence on individual wave characteristics (Blenkinsopp and Chaplin, 2008; Johnson, 2009; Mead and Black, 2001).

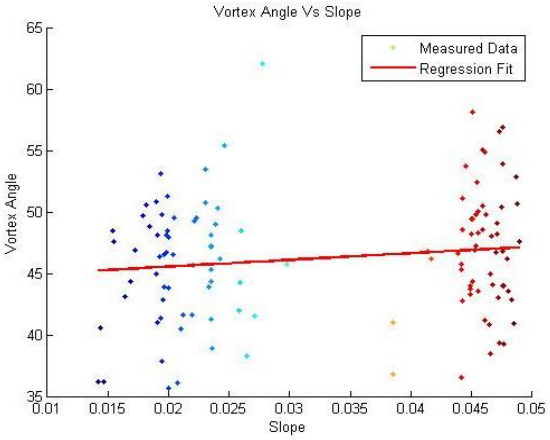

Figure 11: Vortex angle vs. effective slope relationship

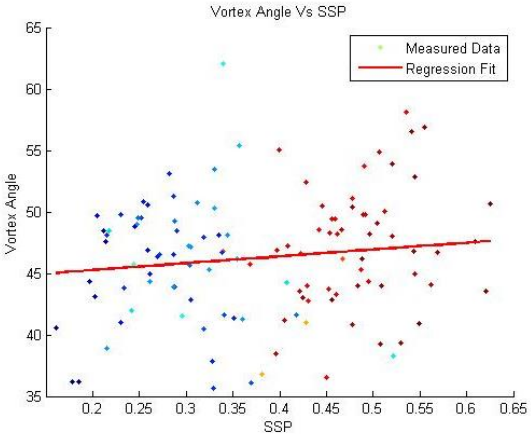

Figure 12: Vortex angle vs. SSP relationship

A multivariable regression analysis was unable to find better correlation than 0.04. Hence, it is concluded that vortex angle is an inappropriate wave characteristic to categorize breaking events. It is suggested that one of the major contributing factors to the lack of angle dependence is a naturally increasing vortex angle, θ, during the progression of the breaking event.

Wave Vortex Parameter Recommendations and Conclusions

Given that the only consistent trend between vortex parameters and wave characteristics was a lack of significant dependence, it is suggested that the use of vortex angle and vortex ratio is insufficient to predict the breaking intensity of waves and should not be investigated further. With the sole exception of Mead and Black (2001), no published studies have found any substantial correlation between these

parameters and breaking conditions, providing evidence to the inconclusive nature of pure vortex ratio or angle descriptions.

However, if further work is completed, it is suggested that the following metrics may provide additional insight into the wave vortex intensity theory (See Figure 13 for visual explanation of suggested parameters). Additionally, a multi-parameter method is recommended.

- Jet Length / Breaker Height Ratio (J_L/H_b): Analysis of Grilli *et al.*'s (1997) profile images shows the jet length/break height ratio changes with seafloor slope.
- Rear Wave Height / Breaker Height Ratio (H_r/H_b): Often qualitatively noted by surfer and ocean enthusiasts, the rear wave height/breaker height may provide additional insight.
- Jet Thickness / Breaker Height Ratio (J_t/H_b) or Jet Area / Breaker Height ^{2} (A_j/H_b^2): Grilli *et al.*(1997) suggested the area of the jet at touchdown may be a good measure of intensity.
- Jet Width / Breaker Height Ratio (J_w/H_b): Given that wave speed in shallow water is directly correlated to depth, the speed differential between the wave jet and the main bulk of the wave will determine the vortex area.

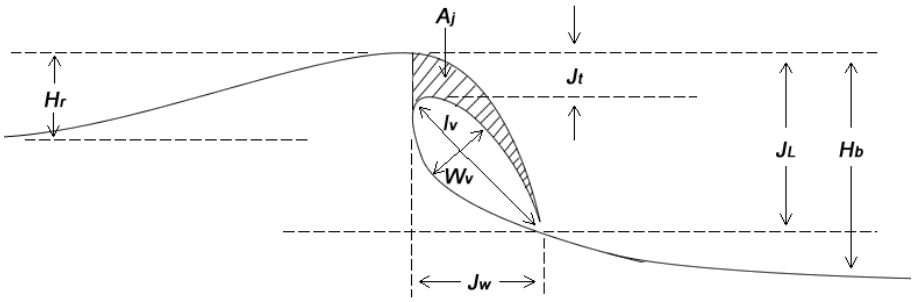

Figure 13: Possible alternate geometric breaking wave description parameters

CONCLUSIONS

The analysis of the shallow water wave breaking phenomenon has been on-going for almost 150 years, and the level of understanding has increased greatly over that time. The collective understanding of wave transformations as they propagate from deep into shallow water, as well as their dissipation within the surf zone has improved steadily. However, the localized effects and processes that effect waves at the instant of breaking are still only vaguely understood. Hence, the measurement and prediction of wave characteristics at the instant of breaking is of paramount importance to any planning or design concerning the surf zone.

This paper presents a novel, low cost (< $350 USD) method to accurately and precisely measure breaking wave characteristics through unified seafloor bathymetric surfaces, directly measured shallow water incoming wave conditions and remote sensing operations. While additional parameters where collected and analyzed in this study, the bulk of the required data point can be collected using a simple off-the-shelf equipment. The final data sets were collected from three independent locations and all excellent resolution and low uncertainty values for all wave characteristics. Breaking heights and positions featured less than 5 % average uncertainty while breaking wave periods featured only 3 % uncertainty.

This study provided quantitative evidence to help improve the performance of breaking wave height and wave characterisation methods:

1. The water depth corrected for optical effects, h_c, resulted in an increased 13 % in predictive performance and is suggested for future optical studies.
2. The effective seafloor slope parameter $m_{1/3}$ was shown to reduce predicted wave height scatter, was more robust to directional uncertainty and improved final breaking wave height predictions by approximately 7.5 %.

3. Crest-to-crest incoming and the proceeding wave period were found to exhibit the highest correlation and are suggested for future use as the best incoming and breaking wave parameters.
4. The exponential wave height prediction form used by Rattanapitikon and Shibayama (2000) and Goda [2010] outperformed all other investigated predictive forms
5. Using the base exponential functional form, an optimized breaking wave height predictor was found to improve R^2 correlations by 8% and 24 % for Rattanapitikon and Shibayama's 2000 equation and Goda's 2010 predictor respectively.
6. No quantifiable or robust trends emerged from detailed analysis of correlations between wave vortex characteristics and standard breaking wave parameters. Only generalized observations could be made; increasing wave heights and breaking depths resulted in lower vortex ratios and decreasing effective seafloor slope resulted in a higher vortex ratios.

Finally, to the best of the author's knowledge, no prior study has collected a more complete and detailed set of irregular breaking wave characteristics in the field. This dataset is now publically available as a resource to assist additional studies in breaking wave conditions.

REFERENCES

Battjes, J.A., 1974. Surf similarity. Proceedings of the International Conference on Coastal Engineering: 466 - 479.

Birkemeier, W.A., Donoghue, C., Long, C.E., Hathaway, K.K. and Baron, C.F., 1997. 1990 delilah nearshore experiment: Summary report. US Army Engineer Waterways Experiment Station, CHL-97-24: 1 - 217.

Black, K. and Rosenberg, M.A., 1992. Semi-empirical treatment of wave transformation outside and inside the breaker line. Coastal Engineering, 16: 313 - 345.

Blenkinsopp, C.E. and Chaplin, J.R., 2008. The effect of relative crest submergence on wave breaking over submerged slopes. Coastal Engineering, 55: 967-974.

CERC-EW, 2008. Coastal engineering manual. EM-1110-2-1100.

Couriel, S., Horton, P. and Cox, D., 1998. Supplementary 2d physical modelling of breaking wave characteristics. Technicial Report, Water Research Laboratory, TR98-14.

de Vries, S., de Schipper, M.A., Hill, D.F. and Stive, M.J.F., 2010. Remote sensing of surf zone waves using stereo imaging. Coastal Engineering: 1 - 12.

Ebersole, B. and Hughes, S., 1986. Duck85 photopole experiment. US Army Engineer Waterways Experiment Station, Misc. Paper CERC-87-8: 1 - 163.

Flick, R.E., Guza, R.T. and Inman, D.L., 1981. Elevation and velocity measurements of laboratory shoaling waves. Journal of Geophysical Research, 86: 4149 - 4160.

Gal, Y., Browne, M. and Lane, C., 2011. Automatic estimation of nearshore wave height from video timestacks. 2011 International Conference on Digital Image Computing: 364 - 369.

Goda, Y., 2010. Reanalysis of regular and random breaking wave statistics. Coastal Engineering Journal, 52(1): 71 - 106.

Grilli, S.T., Svendsen, I.A. and Subramanya, R., 1997. Breaking criterion and characteristics for solitary waves on slopes. Journal of Waterway, Port, Coastal and Ocean Engineering, 123(3): 102 -112.

Johnson, C.M., 2009. The effect of artificial reef configerations on wave breaking intensity relating to recreational surfing conditions. MSc Thesis, Civil Engineering, University of Stellenbosch: 1 - 137.

Kamphuis, J.W., 1991. Incipient wave breaking. Coastal Engineering, 15: 185 - 203.

Khayyer, A., Gotoh, H. and Shao, S.D., 2008. Corrected incompressible sph method for accurate water-surface tracking in breaking waves. Coastal Engineering, 55: 236-250.

Le Mehaute, B., 1976. An introduction of hydrodynamics and water waves. Springer-Verlag.

Lin, P., Philip, L. and Liu, F., 1998. A numerical study of breaking waves in the surf zone. Journal of Fluid Mechanics, 259(239 - 264).

Lippmann, T.C. and Holman, R.A., 1991. Phase speed and angle of breaking waves measured with video techniques. ASCE Coastal Sediments: 542-556.

Longuet - Higgins, M.S., 1982. Parametric solutions for breaking waves. Journal of Fluid Mechanics, 121: 403 - 424.

Longuet - Higgins, M.S. and Stewart, R.W., 1963. A note on wave set-up. Journal of Marine Research, 21(1): 4-10.

Mase, H. and Iwagaki, M., 1982. Wave height distributions and wave groupingh in surf zone. Coastal Engineering: 58-76.
McCowan, J., 1894. On the highest waves of a permanent type. Philosophical Magazine, Edinburgh, 38(5): 351 - 358.
Mead, S.T. and Black, K., 2001. Predicting the breaking intensity of surfing waves. Special Issue of the Journal of Coastal Research on Surfing.: 103 -130.
Ostendorf, D.W. and Madsen, O.S., 1979. An analysis of longshore current and associated sediment transport in the surf zone. Report No. 241, Department of Civil Engineering, MIT: 169.
Rasband, W.S., 1997 - 2012. Imagej. U.S. National Institutes of Health, Bethesda, Maryland, USA.
Rattanapitikon, W. and Shibayama, T., 2000. Verification and modification of breaker height formulas. Coastal Engineering Journal, 42(4): 389 - 406.
Robertson, B., 2013. Remote measurement and analysis of shallow water breaking wave characteristics, University of Guelph.
Robertson, B., Hall, K., Nistor, I. and Zytner, R., 2013a. Breaking waves: Review of characteristic relationships. Coastal Engineering Journal, 1(55): 40.
Robertson, B., Hall, K., Nistor, I., Zytner, R. and Storlazzi, C., 2013b. Remote sensing of irregular breaking wave parameters in field conditions. Journal of Coastal Research: 29.
Rosati, J.D., Gingerich, K.J. and Kraus, N.C., 1990. Superduck surf zone sand transport experiment. US Army Engineer Waterways Experiment Station, CERC - 90-10: 1-75.
Seyama, A. and Kimura, A., 1988. The measured properties of irregular wave breaking and wave height change after breaking on a slope. Proceedings 21th Conference of Coastal Engineering, ACSE: 419 - 432.
Shand, T.D., Bailey, D.G. and Shand, R.D., 2012. Automated detection of breaking wave height using an optical technique. Journal of Coastal Research.
Smith, E.R. and Kraus, N.C., 1991. Laboratory study of wave breaking over bars and artificial reefs. Journal of Waterway, Port, Coastal and Ocean Engineering, 117(4): 307 - 325.
Weggel, R., 1972. Maximum breaker height for design. Proceedings of the International Conference on Coastal Engineering: 419 - 432.